Kinetics and Catalysis, Vol. 44, No. 5, 2003, pp. 682–691. Translated from Kinetika i Kataliz, Vol. 44, No. 5, 2003, pp. 744–754.

CATALYTIC REACTION MECHANISMS

Role of Bifunctionality of ZrO_2-Based Oxide Systems in NO Reduction with Lower Hydrocarbons

S. N. Orlik, V. L. Struzhko, T. V. Mironyuk, and G. M. Tel'biz

Pisarzhevskii Institute of Physical Chemistry, National Academy of Sciences of Ukraine, Kiev, Ukraine

Received December 28, 2002

Abstract—The catalytic properties of transition metal oxides (Cr, Ce, and Co) supported on ZrO_2 synthesized by various methods, as well as the effect of rhodium on the performance of the Me_xO_y/ZrO_2 oxide systems in NO reduction with hydrocarbons (methane, propane–butane mixture, and propene) were studied. The acidity of the surface of the catalysts was studied by IR spectroscopy and ammonia temperature-programmed desorption. The adsorption of NO, propene, and their mixture on the $Rh–Cr_2O_3/ZrO_2$ and $Rh–CeO_2/ZrO_2$ catalysts at temperatures of 293–623 K was studied by IR spectroscopy. The adsorption and co-adsorption of the reactants was found to differ significantly depending on the nature of the surface. The activity of the catalysts studied in NO selective catalytic reduction with hydrocarbons is due to the presence of the acidic functional groups on their surface.

INTRODUCTION

One of the most efficient methods for neutralization of nitrogen oxides NO_x in exhaust gases is catalytic reduction with various reducing agents (CO, NH_3, and C_nH_m), which provides comprehensive cleaning. By now zeolite catalytic systems for the selective catalytic reduction (SCR) of nitrogen oxides with low hydrocarbons $C_1–C_4$ ($NO_x–C_nH_m/O_2$) have been developed and studied worldwide. Although numerous zeolite catalysts have been patented, no commercial sulfur-resistant catalysts for this process are available because of their hydrothermal deactivation. The deactivation can be avoided by the use of the oxide or zeolite–oxide systems. Zirconium dioxide is one of the promising oxide systems and is widely applied as a catalyst and efficient support in heterogeneous catalytic reactions [1–3]. Now the ZrO_2-based catalysts are widely studied in the selective catalytic reduction of nitrogen oxides with various reducing agents (CO, NH_3, and C_nH_m) [4–6]. Rhodium additives substantially enhance the activity of the supported three-way catalysts for the $NO_x/CO/C_nH_m$ transformations because of the ability of rhodium to increase NO conversion due to the dissociation of nitrogen monoxide over rhodium [4, 7].

As is well known, the preparation conditions affect the composition, texture, and crystal structure of zirconium dioxide, resulting in changes in the catalytic properties of ZrO_2 [3, 8].

Active catalysts for NO SCR with hydrocarbons, in particular zeolite catalysts, contain acid sites and sites capable of participating in a redox cycle [9, 10]. The modification of zirconium dioxide is known to alter substantially its acidic properties [11, 12]. The acidic properties of the oxide catalysts for SCR were reported in [13, 14]. In these papers, zirconium dioxide modified with the transition metals (Cu and Mn) was used as a catalyst. It is the acidic properties of sulfated ZrO_2 and the redox properties of the transition metal that provide for the SCR performance of the catalysts.

In this work, the catalytic properties of rhodium-promoted zirconium oxide synthesized by various methods and containing transition metal (Cr, Co, and Ce) oxides introduced by impregnation were studied in NO_x reduction with hydrocarbons C_1, $C_3–C_4$ (methane, propane-butane mixture, and propene) in the presence of sulfur dioxide. The surface acidity of the rhodium-promoted zirconium oxide catalysts ($Rh–Cr_2O_3/ZrO_2$ and $Rh–CeO_2/ZrO_2$) was studied by ammonia temperature-programmed desorption (TPDA) and IR spectroscopy (pyridine adsorption). The adsorption of NO, propene, and their mixture on these catalysts at temperatures of 293–623 K was studied by IR spectroscopy to reveal possible reaction intermediates and their relation to the catalytic activity.

EXPERIMENTAL

Pure zirconium dioxide was prepared by the precipitation and sol–gel method. In the first case, zirconium hydroxide was precipitated from a stirred aqueous solution of zirconium oxochloride with 2.5 M solution of ammonia at a temperature of 293 K and a constant pH of 9. After precipitation, $Zr(OH)_4$ contacted with a mother liquor for 5 days, was washed with ammonia water with (pH 8) until a negative reaction for Cl^- ions, and dried at a temperature of 443 K for 3–4 h. It follows from XRD data that the monoclinic modification of zirconium dioxide (2θ = 28.43 and 31.71 Å) is formed upon $Zr(OH)_4$ thermal treatment.

Another sample of ZrO_2 was prepared by hydrolysis of zirconium isopropoxide in a water–alcohol solution

0023-1584/03/4405-0682$25.00

in the presence of NH_4OH as a catalyst. Water and the organic solvent were removed from zirconia hydrogel by drying in air at a temperature of 423 K. According to XRD data, the tetragonal modification of zirconium dioxide (2θ = 30.57 Å) is formed upon the thermal treatment of $Zr(OH)_4$ at a temperature of 773 K.

Catalysts were prepared by the impregnation of ZrO_2 synthesized by both methods with solutions of the corresponding salts (cobalt and chromium nitrates and cerium chloride) followed by drying at 373 K and calcination at 593 K for 6 h. The catalysts of the Me_xO_y/ZrO_2 composition containing 5 and 10 wt % of transition metal oxides on the support based on the metal were prepared.

The cerium-, cobalt-, and chromium-containing samples were promoted with small quantities of rhodium (0.5 wt %). Rhodium was introduced by impregnation with a solution of rhodium nitrate followed by drying and calcination of the samples.

The catalytic activity of the prepared catalysts in the selective catalytic reduction of $NO–(C_3H_8–C_4H_{10})/O_2$ was characterized by NO conversion to N_2/N_2O, which was measured in a gradientless reactor in the temperature range of 523–773 K in the reaction mixtures of the composition (vol %): 0.05% NO + 0.09% C_nH_m + 5% O_2 + He (Ar) at the gas flow space rate $V_0 = 6000\ h^{-1}$. The concentration of NO was measured on a 344-KhL-04 gas analyzer with a chemiluminescence detector; N_2, N_2O, CO, CO_2, and hydrocarbons were analyzed by chromatography. In separate runs, the effect of sulfur dioxide on the catalytic activity was studied by the addition of up to 0.02 vol % SO_2 to the reaction mixture.

The acidic properties of the catalyst surface were studied by TPDA and IR spectroscopy according to the following procedures [15]. Samples with grains of 1–2 mm (0.2 g) were loaded into a flow reactor (d = 0.6 cm) and treated in a helium flow (v = 60 ml/min) for 1 h at 823 K. After the temperature was decreased to 373 K, the sample was saturated with ammonia. The completion of saturation was checked by titration with ammonia at the outlet of the reactor. The saturated sample was purged with helium at 373 K for 30 min to remove physically adsorbed NH_3. Then the sample was subjected to programmed heating in a helium flow with a ramp of 26 K/min. Thermal desorption was monitored with a thermal conductivity detector, and the amount of desorbed ammonia was estimated by titration with HCl.

Thoroughly dried pyridine was adsorbed on the samples, previously evacuated at 823 K, at a temperature of 423 K for 20 min, and then the samples were evacuated at the same temperature to remove physically adsorbed pyridine. The IR spectra were recorded on a Specord 751R spectrophotometer (Zeiss, Germany).

To study the adsorption of NO, propene, and their mixture by IR spectroscopy, the catalysts were prepared as pellets with a density of 2–3 mg/cm^2 and placed in a special cell. The cell design allowed the thermal vacuum treatment of the catalysts and feeding of the reactants without a change in the sample position in the cell. Before measurements, the catalysts were thermally evacuated at a temperature of 823 K and a pressure of 10^{-4} Torr for 2 h, and then the temperature was reduced to 293 K. NO, propene, and their mixture were adsorbed by specified volumes of the adsorbates on the surface of the pretreated samples at temperatures of 293 and 373 K. Excess gaseous products were removed from the cell by controlled evacuation.

The X-ray photoelectron spectra of the sample surface were recorded on a SERIES-800XPS spectrophotometer. The spectra were calibrated by the C1*s* line of the adsorbed hydrocarbons. The excitation X-ray radiation energy was 1486.6 eV. The samples were prepared for the XPS measurements according to a standard procedure [16].

The electron microscopic study of the Rh–Me_xO_y/ZrO_2 samples was carried out using a REM-100U scanning electron microscope.

RESULTS AND DISCUSSION

The initial ZrO_2 samples prepared by both methods and samples containing 5 and 10 wt % CeO_2/ZrO_2 were inactive in the reaction under study in the temperature range up to 723 K. The lack of the activity of a series of oxides including ZrO_2 in the presence of the active reducing agents (C_2H_4 or C_3H_6) has been noticed in the review [17]. Under our experimental conditions, the catalyst 10% CeO_2/ZrO_2 is active in the oxidation of a propane–butane mixture with oxygen. The conversion of $C_3–C_4$ hydrocarbons reaches 5–60% in the temperature range of 250–500°C (0.09% $C_3–C_4$ + 5% O_2 + He; $V = 6000\ h^{-1}$).

Zirconia-supported cobalt and chromium oxide catalysts are active in NO SCR with a propane–butane mixture, and their activity depends on the procedure of zirconium dioxide preparation. The NO conversion to nitrogen on the most active sample of 10% Cr_2O_3/ZrO_2 (ZrO_2 was prepared through the alkoxide gel stage) reaches 54% at 573 K. In the presence of sulfur dioxide in the reaction mixture, NO conversion even increases and reaches 60% in the temperature range of 573–633 K [18]. The reason for the activity increase can be the sulfate formation, as sulfated zirconium dioxide is known to exhibit the solid superacid properties and catalyzes NO SCR with hydrocarbons [19].

To elucidate the reason for the dependence of the catalytic activity of the samples on the preparation procedure, we studied the surface acidic properties of the zirconium catalysts modified by chromium oxide by TPDA and IR spectroscopy. The concentration of the acid sites in the initial ZrO_2 samples prepared by different methods is high (0.13 and 0.23 mmol/g, Table 1), but they are inactive, whereas the sample of 10% Cr_2O_3/ZrO_2 prepared by the sol–gel method is very active in this reaction at the same surface acidity (Table 1). The sample of a similar composition prepared

Table 1. Activity of ZrO_2 and M_xO_y/ZrO_2 in NO SCR with hydrocarbons C_nH_m and their acidity studied by TPDA

Catalyst	Procedure of ZrO_2 preparation	NO conversion, %	T, °C	C_nH_m	Concentration of acid sites, mmol NH_3/g
ZrO_2	Precipitation	Inactive	<400	–	0.13
ZrO_2	Sol–gel	″	″	–	0.23
10% Cr_2O_3/ZrO_2	Precipitation	13	300	C_3–C_4	0.05
10% Cr_2O_3/ZrO_2	Sol–gel	54 (60 with SO_2)	″	″	0.13
10% CoO/ZrO_2	Precipitation	75	310	CH_4	0.12
10% CoO/ZrO_2	Sol–gel	72	300	″	–
10% CeO_2/ZrO_2	Precipitation	Inactive	<400	″	–

Note: 0.05% NO + 0.09% C_nH_m + 5% O_2; V_0 = 6000 h^{-1}.

Table 2. Results of the study of the Rh–M_xO_y/ZrO_2 catalysts by X-ray photoelectron spectroscopy

Catalyst	Bond energy of photoelectrons, eV					
	Rh3*d*	Zr3*d*	O1*s*	Ce3*d*	Cr2*p*	Co2*p*
Rh–CeO_2/ZrO_2	308.3	182.3	530.3	883.1	–	–
Rh–Cr_2O_3/ZrO_2	″	″	530.4	–	577.1	–
Rh–CoO/ZrO_2	308.5	182.5	″	–	–	781.9
[22]*	″ (Rh (I))	182.6 (Zr^{4+})	530.7 (ZrO_2)	882.1 (CeO_2)	576.8 (Cr_2O_3)	780.0 (CoO)

* Reference data on the bond energies of photoelectrons in the corresponding compounds.

by precipitation has a 2.5 times lower SCR activity. These findings confirm that the catalytic activity in NO_x SCR with hydrocarbons is determined by both the surface acidity and the active metal concentration.

Figure 1a presents the medium-region (400–1200 cm^{-1}) IR spectra of the zirconium dioxide samples prepared by the sol–gel method and modified with 10% Cr_2O_3. As is seen from the figure, the modification of zirconium oxide with chromium oxide results in the appearance of local vibrations in the IR spectra, which are not the intrinsic vibration modes of the lattices of the zirconium and chromium oxides. The presence of the absorption bands at 800, 1025, and 1170 cm^{-1} in the spectrum of sample 2 may indicate the formation of new Zr–O–Cr metal–oxygen bonds in the subsurface layer of zirconium dioxide.

Figure 1b shows the IR spectra of pyridine adsorbed on the previously dehydrated samples. In the spectrum of initial zirconium dioxide prepared from the alkoxide gel, the absorption band typical of the Brønsted acid sites is absent. The absence of the Brønsted acid sites on the surface of tetragonal ZrO_2 were observed in [20] by IR spectroscopy of adsorbed pyridine. When chromium dioxide is introduced in zirconium dioxide acid sites appear corresponding to the absorption band at 1540 cm^{-1} typical of the pyridinium ions. This is likely due to the formation of bridging structures [3]:

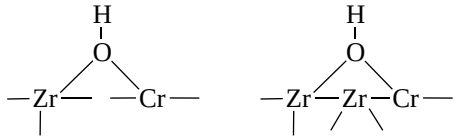

It has been shown earlier [15] that the activity of the Cu-, Ce-, and Co-containing pentasils in the SCR of nitrogen oxides with C_1–C_4 hydrocarbons correlates with the strength of the Brønsted acid sites. We explained this correlation by the fact that it is the Brønsted acid sites on which the activation of the reducing hydrocarbon occurs [21]. The findings of this work confirm an important role of the Brønsted acid sites in the reaction under study over the ZrO_2-based oxide systems.

To estimate the composition and the valence state of elements in the ZrO_2-based catalysts, they were studied by XPS. The results are shown in Table 2. The intense lines with a binding energy of 182.3 (182.5) eV typical of Zr^{4+} were found in the spectra of all the samples. In the X-ray photoelectron spectra of the active phase of the samples of Rh–M_xO_y/ZrO_2 (M = Cr, Ce, and Co) (Table 2), the intense lines from Cr2*p* (577.1 eV), Ce3*d* (883.1 eV), and Co2*p* (781.9 eV) electrons are found typical of the Cr^{3+}, Ce^{4+}, and Co^{2+} ions, which are affected by the electron-acceptor influence of ZrO_2. Substantial positive shifts of the binding energies compared to those in the corresponding oxides Cr_2O_3

(576.8 eV), CeO_2(882.1 eV), and CoO (780.0 eV) confirm this effect. In the spectra of Rh3*d* electrons in the samples, the lines with 308.3 (308.5) eV typical of Rh(I) with a binding energy of ~308.5 eV have been found [22].

The SEM images of the catalyst samples indicate a developed surface area and its uniformity in all the samples with the minimal particle size in the supported catalyst at the level of 0.5 μm (5000 Å). These data agree with the specific surface areas determined from the argon thermal desorption (Table 3).

Table 3 presents data on the activity of the Rh-promoted catalysts compared with the nonpromoted samples in NO SCR with C_3–C_4 hydrocarbons (propane–butane mixture). It is seen that doping with rhodium increases the activity of ZrO_2-based oxide catalysts in selective reduction: the NO conversion increases over the chromium–zirconia and cobalt–zirconia catalysts, and the cerium–zirconia sample becomes catalytically active (the conversion is 8% at 683 K).

When oxygen is absent from the reaction mixture (Tables 3, 4), almost complete NO conversion is observed over all the Rh-promoted catalysts in the whole temperature range (523–773 K). Nitrogen and nitrous oxide (45–90% N_2O) are the reduction products. Propane–butane mixture partially transforms to CO_2 (up to 10%) and the products of incomplete oxidation, including methanol, ethanol, butanol, propionic acid, and butyric aldehyde, which were identified by chromatography. That is, in the absence of oxygen, NO is a mild oxidant for hydrocarbons and is reduced to nitrogen and/or nitrous oxide.

The fact that most NO_x transforms into N_2O more rapidly than to N_2 is the main drawback of the platinum group metals as catalysts for the reduction of nitrogen oxides. Nitrogen is formed through the recombination of two adsorbed N atoms, and N_2O is formed by the reaction of the adsorbed NO molecule with the N atom, i.e., the selectivity (N_2/N_2O) of the rhodium-containing catalysts is controlled by the bimolecular reaction $NO_{ads} + N_{ads}$ [23]. The results obtained agree with the previously reported data that oxygen retards NO reduction with various reducing agents (CO and hydrocarbons) over noble metals, in particular, over rhodium [24]. The reasons for such retardation can be the concurrent adsorption of nitrogen monoxide and oxygen on the same active sites as well as the competition between two oxidants, NO and O_2, for the reducing agent, hydrocarbon. As a result, the reaction $C_nH_m + O_2 \Rightarrow CO_x + H_2O$ prevails over the reaction $C_nH_m + NO \Rightarrow N_2 + CO_x + H_2O$.

Table 4 presents data on NO reduction with various hydrocarbons. A comparison of NO SCR with a propane–butane mixture and propene shows that the conversion is higher upon reduction with alkene. This fact is in agreement with the earlier data and our findings on the higher reactivity of alkenes compared to alkanes in this process over cation-exchanged zeolites [25, 26].

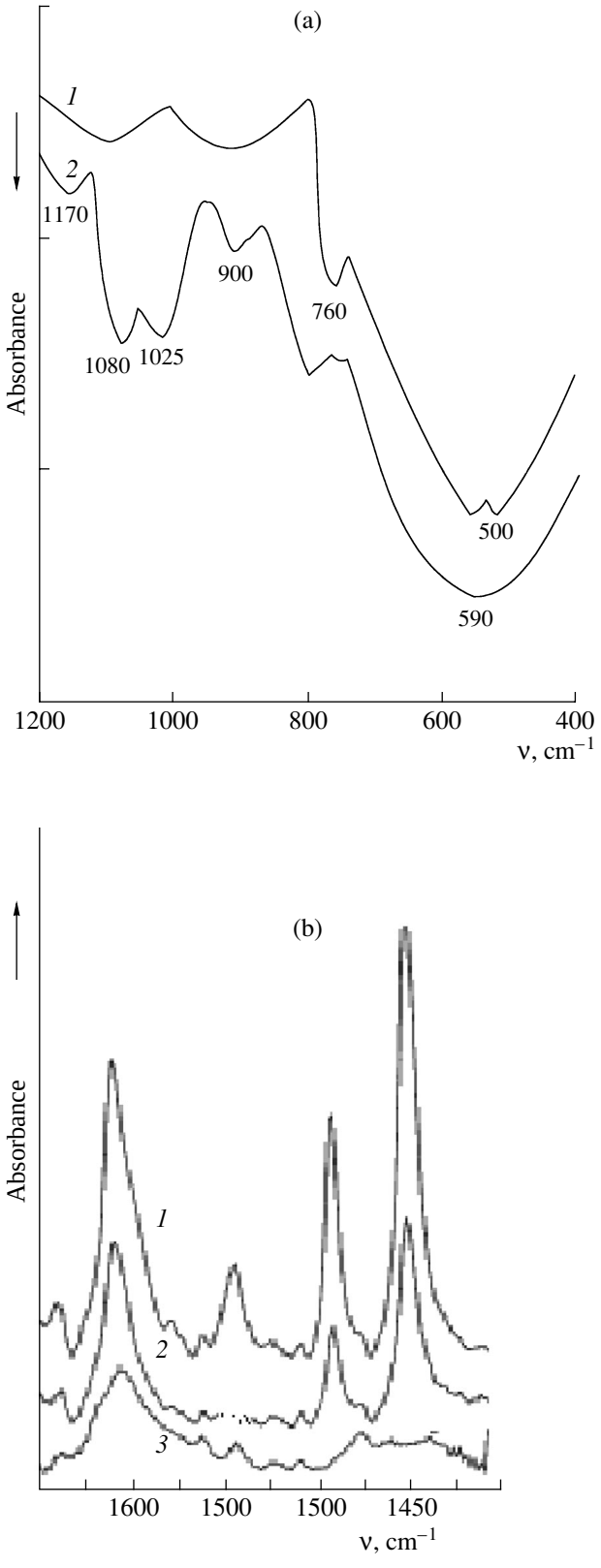

Fig. 1. IR spectra of samples prepared by the sol–gel method. (a) in the medium IR region: (*1*) ZrO_2 and (*2*) 10% Cr_2O_3/ZrO_2; (b) (*3*) after thermal vacuum treatment of ZrO_2 at 823 K; (*2*) after pyridine adsorption on ZrO_2; and (*1*) on 10% Cr_2O_3/ZrO_2.

Table 3. Effect of rhodium on the activity of the M_xO_y/ZrO_2 catalysts in NO reduction with C_3–C_4 hydrocarbons

Catalyst	Procedure of ZrO_2 preparation	S, m^2/g	Maximal conversion of NO, % (T, °C)	
			NO + C_3–C_4 + O_2	NO + C_3–C_4
Rh–Cr_2O_3/ZrO_2	Sol–gel	85	59 (310)	97–99 (250–500)
10% Cr_2O_3/ZrO_2	″	″	54 (300)	Inactive
Rh–CeO_2/ZrO_2	Precipitation	112	8 (410)	95–97 (250–500)
10% CeO_2/ZrO_2	″	″	Inactive	Inactive
Rh–CoO/ZrO_2	Precipitation	109	51 (300)	96–98 (250–500)
5% CoO/ZrO_2	″	″	40 (300) 72* (300)	Inactive

Note: 0.05% NO + 0.09% C_3H_8–C_4H_{10} + (5% O_2) + Ar; V = 6000 h^{-1}.
* NO conversion in reduction with methane.

Table 4. Effect of reducing agents on NO conversion over the rhodium-promoted oxide systems M_xO_y/ZrO_2 (0.05% NO + 0.09% C_nH_m + 5% O_2 + Ar; V = 6000 h^{-1})

Catalyst	NO conversion, % (T, °C)					
	C_3–C_4 + NO	C_3–C_4 + NO + O_2	C_3H_6 + NO	C_3H_6 + NO + O_2	CH_4 + NO	CH_4 + NO + O_2
Rh–Cr_2O_3/ZrO_2	97–99 (250–500)	59 (310)	99 (250–500)	67 (280)	Inactive 450°C	72 (300) NO + O_2 72 (300)
Rh–CeO_2/ZrO_2	95–97 (250–500)	8 (410)	97–99 (250–500)	21 (360)	Inactive 450°C	20 (360)
Rh–CoO/ZrO_2	96–98 (250–500)	51 (300)	99 (250–500)	59 (300)	34–67 (300–475)	41 (300)

This can be due to the higher energies of the R–H bond rupture in alkanes compared to alkenes: C_3H_7–H (410 kJ/mol) > C_3H_5–H (361 kJ/mol). The opposite change in the activity when the R–H bond energy in the hydrocarbon molecule changes suggests that the rate-determining stage of SCR involves the activation of hydrocarbon as a reducing agent by the dissociation of the R–H bond.

Figure 2a shows the temperature dependence of the reaction rate of selective NO reduction with propene and a propane–butane mixture over the most active catalyst Rh–Cr_2O_3/ZrO_2. The appearance of extremums on the plot for the reaction rate vs. temperature for C_3 hydrocarbons can be explained by the fact that a side reaction, the complete oxidation of hydrocarbon with oxygen to CO_2, begins to prevail with an increase in temperature. When NO is reduced with methane, NO transforms to nitrogen (nitrous oxide) only over the cobalt-containing catalyst, whereas over the chromium- and cerium-containing samples, NO is oxidized with oxygen to NO_2 (Table 4). As is seen from Fig. 2b, the temperature dependence for NO conversion (X_{NO}) is nearly the same for the reaction mixtures NO + O_2 and CH_4 + NO + O_2. The curves pass below the calculated equilibrium curve for the reaction $2NO + O_2 \Rightarrow 2NO_2$. When oxygen is absent from the reaction mixture CH_4 + NO, the conversion of nitrogen monoxide was not found over both catalysts (chromium- and cerium-containing) up to a temperature of 723 K (Table 4).

To explain the differences in the activity of the rhodium-promoted oxide catalysts (chromium- and cerium-zirconia), we studied the surface acidic properties of the samples. Figure 3 shows the IR spectra of pyridine adsorbed on the samples of Rh–Cr_2O_3/ZrO_2 (sample **1**) and Rh–CeO_2/ZrO_2 (sample **2**). In the case of Rh–Cr_2O_3/ZrO_2, the absorption bands typical of the pyridinium ion (1637 and 1545 cm^{-1}) appear in the spectrum, indicating the presence of the Brönsted acid sites on the sample surface [27]. The absorption bands for sample **1** (1620, 1490, and 1440 cm^{-1}) characterize, according to [27], the formation of pyridine sorption complexes with the electron-acceptor sites of the catalysts. Similar absorption bands were found for the nonpromoted sample Cr_2O_3/ZrO_2 [18]. In the case of Rh–CeO_2/ZrO_2, the absorption bands were not found in the cited region, and this may indicate a significantly lesser amount of the acidic functional groups on the surface of this catalyst.

The surface acidic properties were also studied by temperature-programmed desorption of ammonia. The results are presented in Table 5 and Fig. 3b. The total concentration of the acid sites in the samples differ by ~3.5 times. The rhodium–chromium–zirconia catalyst has weak and strong acid sites (**A** and **B**, respectively)

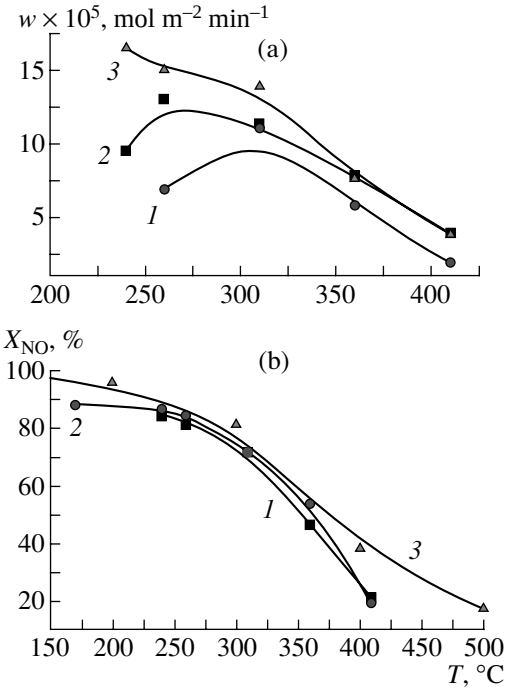

Fig. 2. Temperature plots for the Rh–10% Cr_2O_3/ZrO_2 sample (a) for the rate of NO SCR in the reaction mixtures of composition (vol %): 0.05% NO + 0.09%C_nH_m + 5%O_2 + Ar; V = 6000 h^{-1} during reduction with (*1*) C_3H_8–C_4H_{10} and (*2*) C_3H_6; (*3*) the rate of NO oxidation to NO_2 in the presence of CH_4; (b) for NO conversion (X_{NO}) in the reaction mixtures of composition (vol %): (*1*) 0.05% NO + 0.09% CH_4 + 5%O_2 + Ar; V = 6000 h^{-1}; (*2*): 0.05%NO + 5%O_2 + Ar; V = 6000 h^{-1}; (*3*) calculated equilibrium curve for the reaction $2NO + O_2 \rightleftharpoons 2NO_2$ in the mixture of 0.05% NO + 6%O_2 composition.

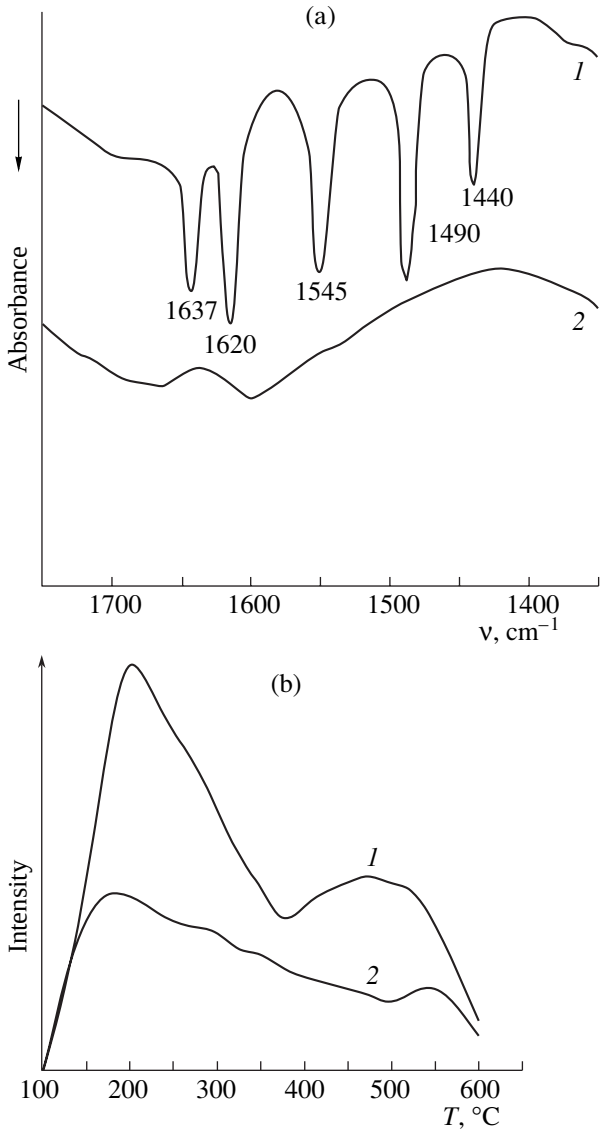

Fig. 3. (a) IR spectra of pyridine adsorbed on samples (*1*) Rh–Cr_2O_3/ZrO_2 and (*2*) Rh–CeO_2/ZrO_2; (b) thermal desorption spectra from the surface of samples (*1*) Rh–Cr_2O_3/ZrO_2 and (*2*) Rh–CeO_2/ZrO_2.

corresponding to the maxima of the thermal-desorption peaks on curve *1* (Fig. 3b). The rhodium–cerium–zirconia is characterized by a smoothed thermal-desorption curve with a small high-temperature maximum at 550°C and a total concentration of the acid sites equal to 0.04 mmol NH_3/g.

The results of the R spectroscopic and TPDA studies of the surface acidity of the catalysts agree with each other and correlate with the catalytic activity of the samples in selective NO reduction with both a propane–butane mixture and propene. The more active catalyst Rh–Cr_2O_3/ZrO_2 contains the strong acid **B**-sites. This means that the active catalyst for NO SCR with C_nH_m should contain active metal (metal oxide) and strong Brønsted acid sites as it was shown by us for the zeolite catalysts [15] and zirconia-based oxide systems ZrO_2 – Me_xO_y/ZrO_2 [18].

To reveal possible surface intermediates in NO reduction with propene and their relation to the catalytic activity, we studied the adsorption of NO, propene, and their mixture on samples **1** and **2** by IR spectroscopy.

NO adsorption. Figure 4a presents the IR spectra of the adsorbed nitrogen monoxide. As can be seen from the figure, the adsorption bands at 1850 and 1660 cm^{-1} appear in the spectrum of NO adsorbed on the sample of Rh–Cr_2O_3/ZrO_2. A shift of the absorption band at 1850 cm^{-1} relative to that of a free nitrogen monoxide molecule at 1880 cm^{-1} [27] can be due to the formation of stable complexes of partially oxidized rhodium cations (Rh–NO^+) on the sample surface due to electron transfer from the $2p\pi^*$ antibonding orbital of the NO molecule to the rhodium 4*d* orbital [28, 29]. The appearance of the absorption band with a maximum at 1660 cm^{-1} can be due to the formation of the complex Rh^0–N=O^- [29]. An increase in temperature to 373 K followed by evacuation does not result in the disappear-

Table 5. Concentration of the acid sites from the data on ammonia thermal desorption over the rhodium-promoted oxide catalysts

Catalyst	Concentration of acid sites, mmol NH_3/g (mmol NH_3/m^2)		
	[**A**], 150–300°C	[**B**], 350–600°C	Σ
$Rh–Cr_2O_3/ZrO_2$	0.08 (9.4×10^{-4})	0.06 (7.05×10^{-4})	0.14 (1.65×10^{-3})
$Rh–CeO_2/ZrO_2$	3.6×10^{-2} (3.21×10^{-4})	4×10^{-3} (3.6×10^{-5})	0.04 (3.57×10^{-4})

Table 6. Spectral characteristics of the CH_x species formed upon C_3H_6 adsorption on the $Rh–M_xO_y/ZrO_2$ catalysts

Vibration mode	ν, cm^{-1}	Reference
$\nu_{as}(=CH_2)$	3060, 3050*	[32]
$\nu_s(=CH_2)$	2970*	[32, 33]
$\nu_{as}(–CH_3)$		[35]
$\nu_{as}(–CH_3)$	2960	[35]
$\nu_s(=CH_2)$		[32]
$\nu_s(–CH_3)$	2930*	[35]
$\nu_{as}(–CH_3)$		[32]
$\nu_{as}(=CH_2)$	2870*	[35]
ν_{as} and/or νs(–CH)		[31]
ν_{as} and/or s(–CH)	2890*	[31]

* Frequencies of propene on the $Rh–Cr_2O_3/ZrO_2$ catalyst.

ance of the absorption bands of adsorbed NO but gives rise to the absorption band at 1440 cm^{-1}, which can be attributed to a nitrito complex (ONO) on the surface of platinum group metals [28].

When NO was adsorbed on the sample of $Rh–CeO_2/ZrO_2$, the broad absorption bands at 1870 and 1640 cm^{-1} disappeared after heating and evacuation, indicating a physical nature of the nitrogen monoxide adsorption.

Propene adsorption. Figure 4b shows the IR spectra of propene adsorbed on samples **1** and **2**. The absorption bands characteristic of the atom vibrations in liquid propene [30] appear in the spectra of both samples. Among them, the bands of symmetric and asymmetric stretching vibrations of the C–H bonds in the CH_2 and CH_3 groups occur (Table 6). The absorption band at 1630 cm^{-1} corresponds to the stretching vibrations of the C=C bonds for the sample $Rh–CeO_2/ZrO_2$, as well as the band at 1650 cm^{-1} for the sample $Rh–Cr_2O_3/ZrO_2$ [31]. Absorption at 1440 cm^{-1} is caused by the bending vibrations of the C–H bonds. The absorption bands at 1465 and 1460 cm^{-1} correspond to the asymmetric bending vibrations of the methyl groups (δ_{as}) [32] in samples **1** and **2**, respectively. The absorption bands at 1380 and 1440 cm^{-1} can be assigned to the allyl species or carboxylate complexes formed with the participation of the surface oxygen of the oxides [28, 33].

After keeping sample **2** for 1 h at a temperature of 293 K, no changes in the spectrum were found. Gradual heating up to 373 K followed by evacuation results in almost complete disappearance of the absorption bands (Fig. 4b, spectrum *2'*), confirming a physical nature of alkene adsorption.

The broad band at 3050 cm^{-1} can indicate the presence of the strong acidic OH groups [18, 34] bound via a hydrogen bond with the alkene molecules on the surface of sample **1** [35]. Note that we failed to determine the presence or absence of the hydroxy groups on the surface because of the strong absorption by the sample in the 3200–4000 cm^{-1} region. Nevertheless, the conversion of the adsorbed propene molecules upon adsorption and subsequent heating confirms the presence of the acidic functional groups on the catalyst surface. After gradual heating and evacuation, the absorption bands typical of propene disappear and the absorption bands at 1600 cm^{-1} arise, indicating the formation of polyene compounds [36], that is, the start of alkene polymerization. An increase in temperature to 623 K followed by evacuation results in the almost complete desorption of products from the catalyst surface.

Adsorption of reaction mixture. The formation of the surface compounds upon the adsorption of the reaction mixture on the sample under study is likely due to the presence of active sites of several types, namely, hydroxy groups, electron-acceptor rhodium ions, and electron-donor oxygen ions.

Figure 4c presents the IR spectra of adsorbed compounds formed on the surface of sample **1** upon adsorption of an NO + C_3H_6 mixture at 293 K followed by heating. As can be seen, the absorption bands in the 1200–1700 cm^{-1} region are found in the IR spectrum at 293 K, which likely relate to the propene complexes with the acid sites of the sample (ν(C=C) = 1640 and 1580 cm^{-1}), namely, the stretching and bending vibrations of CH and CH_2 groups of propene. Upon alkene adsorption, we found neither absorption bands in the regions of 1250 and 1570 cm^{-1} nor the broadening of the band at 1640 cm^{-1}. Therefore, they can be attributed to the vibrations of both –NCO and other reaction intermediates [28, 29].

An increase in temperature to 373 K substantially changes the spectrum. A decrease in the intensity of the absorption bands with maxima at 1250, 1570, and 1640 cm^{-1} likely gives evidence for the occurrence of the surface reactions of the above intermediates. Note that the presence of strong acid sites on the surface can lead to oligomerization followed by polymerization of a fraction of alkene as shown by the appearance of absorption bands at 1600 and 1320 cm^{-1} in the spectrum. Upon adsorption of a reaction mixture NO + C_3H_6 on the surface of sample **1** at a temperature of 373 K, the absorption band at 1870 cm^{-1} is observed.

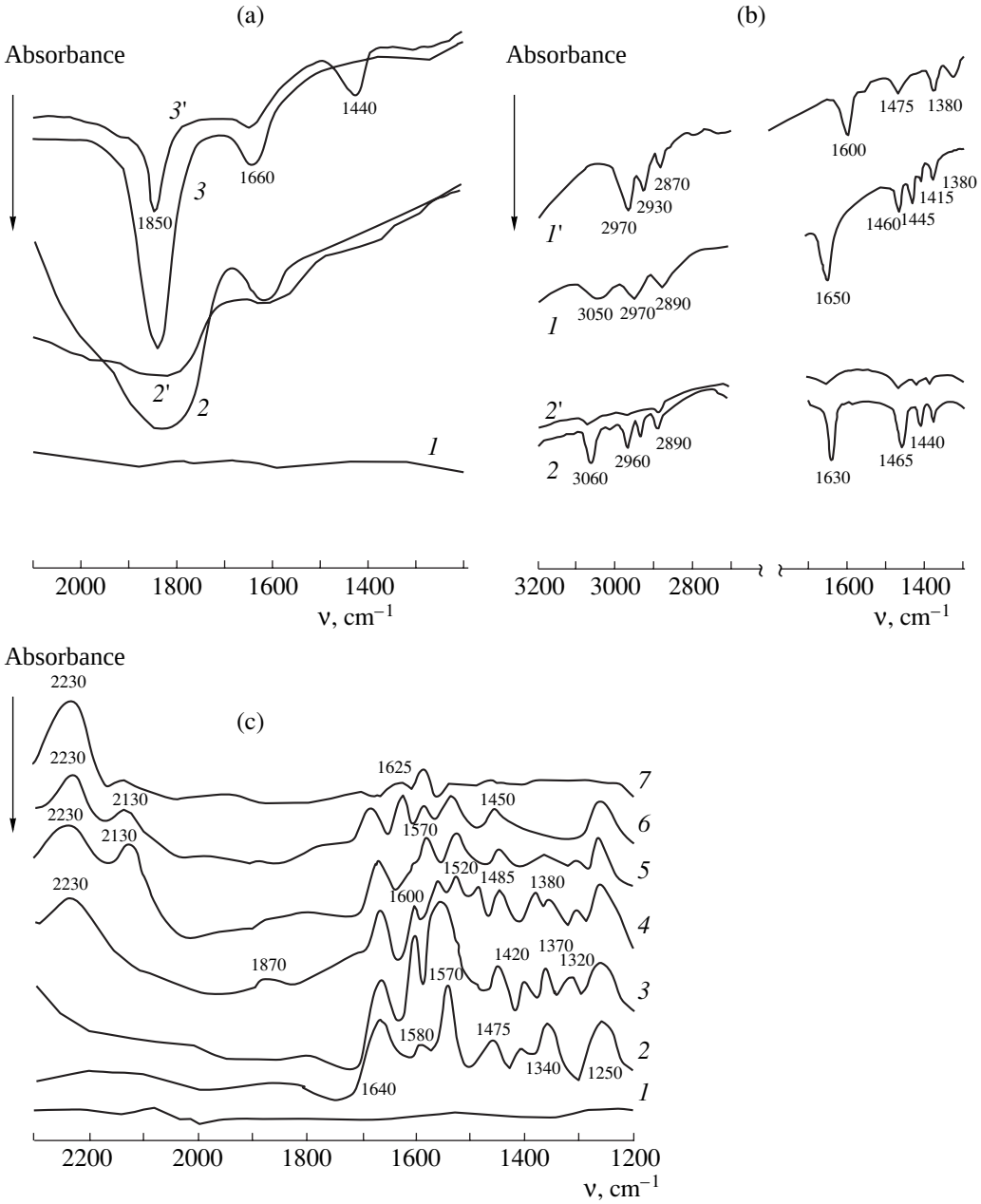

Fig. 4. IR spectra: (a) of nitrogen monoxide adsorbed on samples (*2*, *2*') Rh–CeO_2/ZrO_2 and the same at 373 K; (*3*, *3*') Rh–Cr_2O_3/ZrO_2 at T = 293 (*2*, *3*) and 375 K (*2*', *3*'); *1*, the background spectrum; (b) of propene adsorbed on samples (*1*, *1*') Rh–Cr_2O_3/ZrO_2 and (*2*, *2*') Rh–CeO_2/ZrO_2 at T = 293 (*1*, *2*) and 373 (*1*', *2*'); (c) of adsorbed compounds formed on the surface of Rh–Cr_2O_3/ZrO_2 (*1*) before and after adsorption of the NO + C_3H_6 mixture at temperatures (*2*) 293, (*3*) 373, (*4*), 473, (*5*) 523, (*6*) 573, and (*7*) 623 K.

The band can be assigned to the vibrations of the Rh–NO^+ bond in agreement with [28, 29].

An increase in the adsorption temperature up to 473 K significantly decreases the intensity of the absorption bands at 1600, 1320, 1570, and 1640 cm^{-1}. At the same time, the absorption bands at 2230 and 1520 cm^{-1} appear in the spectrum, which are likely due to the decomposition or further reactions of surface compounds.

The presence of the active sites on the surface, including the coordinatively unsaturated metal ions, nucleophilic oxygen ions, and hydroxyl groups, is known to be sufficient for the formation of π-allyl complexes [35]. In this connection, the absorption bands at 1570 and 1320 cm^{-1} can be due to the C=C–C bonds of the π-allyl complex. Note that these bands were also seen at 293 K. When the temperature is increased up to 523 K, the absorption bands at 2120 cm^{-1} appear in the

high-frequency region of the spectrum. The temperature dependence (Fig. 4c, spectra *5*, *6*) and the intensity growth (absorption bands at 2120 and 2230 cm^{-1}) with the simultaneous decrease in the intensity of the other bands allow us to assign these bands to the formation of the surface nitrile (–CN) and isocyanate (–NCO) species. Note that the allyl complexes formed on the catalyst surface with the participation of the active sites are precursors for the above complexes. The absorption bands of the allyl complexes as well as that at 1870 cm^{-1} disappear in the spectrum in the temperature range of 473–523 K when the active surface intermediates, the nitrile and isocyanate structures, are formed.

The adsorption of the reaction mixture on sample **2**, unlike that on sample **1**, did not lead to the formation of any strongly bound compounds under similar conditions, and the physically adsorbed molecules of the mixture were readily removed from the subsurface layer by evacuation.

The above results allow us to consider a possible mechanism of the reaction NO + $C_3H_6(+O_2)$ mediated by the proton-donor surface sites (strong acid **B**-sites) [34] to form the strongly bound adsorbed propene compounds ($-C_3H_5$, π-C_3H_5, polyene species) and rhodium atoms with the adsorbed surface NO complexes followed by the formation of the $Rh–NO^+$ species. Then this species reacts with propene and/or other adsorbed species (π-C_3H_5, polyene) to form the isocyanate complexes Rh–NCO. The interaction of these complexes with oxidizing agents (O_2, NO, and NO_2) under the conditions of SCR gives rise to the reaction products: N_2, N_2O, and CO_2. Taking into account the above data and the data of [28, 31], we can suggest the following mechanism of the selective NO reduction with propene:

$$Rh^+ + NO \rightleftharpoons Rh–NO^+,$$

$$C_3H_{6(g)} \longrightarrow C_3H_{6(ads)} \longrightarrow \pi\text{-}C_3H_5,$$

$$Rh–NO^+ + \pi\text{-}C_3H_5 \longrightarrow Rh–NCO,$$

$$Rh–NCO + NO\ (O_2, NO_2) \longrightarrow N_2, N_2O, CO_2.$$

In our opinion, rhodium plays the main role in the nonselective nitrogen monoxide reduction, and NO dissociation to N and O atoms, when O_2 is absent as the competitive oxidizing agent, occurs on Rh atoms. In [37], the main elementary steps of NO decomposition on rhodium have been identified: $NO_{(g)} \longrightarrow NO_{(ads)} \longrightarrow N_{(ads)} + O_{(ads)} \longrightarrow N_{2(g)} + O_{2(g)}$. The atomic oxygen formed can activate hydrocarbon to form partial oxidation products (alcohols, acids, and aldehydes). Hence, in the absence of oxygen, NO is a mild oxidant for hydrocarbons on both rhodium-containing catalysts and is reduced to nitrogen and/or nitrous oxide (Tables 3, 4). In the case of $Rh–CeO_2/ZrO_2$, the redox pair Ce^{3+}/Ce^{4+} plays an important role and its effect is due to the stabilization of the surface oxygen vacancies and oxygen accumulation: $Ce^{3+} + NO \longrightarrow Ce^{4+}\cdot\cdot O + 1/2N_2$ [38, 39].

Hence, adsorption and co-adsorption of reactants (NO + C_3H_6) differ substantially depending on the nature of the rhodium-doped complex oxide systems M_xO_y/ZrO_2. The reason for weak adsorption interactions in the reaction mixture on the surface of the $Rh–CeO_2/ZrO_2$ sample at temperatures close to those of catalysis is the absence of the functional groups of the acid nature on the surface [34]. This results in the significantly lower activity of this catalyst in NO selective reduction with propene.

CONCLUSIONS

(1) The activity of the ZrO_2-based oxide catalysts (Co-, Cr-, and Ce-containing) in the SCR of nitrogen oxides with hydrocarbons depends on the preparation procedure for zirconium dioxide; the samples based on ZrO_2 (tetragonal modification) prepared by the sol–gel method were the most active; it was shown by TPDA and IR spectroscopy that the most active catalyst is characterized by the presence of strong Brønsted acid sites.

(2) The doping of the oxide systems M_xO_y/ZrO_2 with rhodium leads to an increase in their activity in NO SCR with the propane–butane mixture. In the nonselective reduction of nitrogen monoxide (in the absence of oxygen) over all the catalysts studied, the almost complete NO conversion is achieved in a temperature range of 523–773 K (selectivity to nitrogen is 10–55% and N_2O is the rest).

(3) The correlation of the activity of zirconia catalysts with the surface acidic properties (strength and type of the acid sites) was found. The adsorption and coadsorption of the reactants (NO and C_3H_6) on the catalysts $Rh–Cr_2O_3/ZrO_2$ and $Rh–CeO_2/ZrO_2$ differ substantially depending on the surface nature (presence of functional acid groups), and this results in the different catalytic activity in NO_x SCR with hydrocarbons.

Hence, it was found by IR spectroscopy and temperature-programmed desorption of ammonia that zirconia systems impregnated with the transition metal oxides, including the rhodium-doped samples, are bifunctional catalysts and their activity in the selective reduction of nitrogen oxides with lower hydrocarbons is determined by the presence of the redox site and strong Brønsted acid sites.

REFERENCES

1. Iwamoto, M., *Stud. Surf. Sci. Catal.*, 2002, vol. 130, p. 23.
2. Fokema, M.D. and Ying, J.Y., *Cat. Rev. – Sci. Eng.*, 2001, vol. 42, nos. 1–2, p. 1.
3. Tanabe, K., *Catalysts and Catalytic Processes*, Moscow: Mir, 1993.
4. Fornasiero, P., Rao, G.R., Kaspar, J., L'Erario, F., and Graziani, M., *J. Catal.*, 1998, vol. 175, no. 2, p. 269.

5. Pietrogiacomi, D., Sannino, D., Tuti, S., Ciambelli, P., Indovina, V., and Occhiuzzi, M., *Appl. Catal., B*, 1998, vol. 21, no. 2, p. 141.
6. Zub Yu., L., Babich, N.N., and Orlik, S.N., *Book of Abstracts*, EuropaCat-, IV., Rimini, 1999, p. 314.
7. Chuang, S.S.C. and Tan, C.D., *J. Catal.*, 1998, vol. 173, no. 1, p. 95.
8. Kharlanov, A.N., Lunina, E.V., and Lunin, V.V., *Zh. Fiz. Khim.*, 1997, vol. 71, no. 9, p. 1672.
9. Amiridis, M.D., Zhang, T., and Farrauto, R.J., *Appl. Catal., B*, 1996, vol. 10, p. 203.
10. Orlik, S.N., *Teor. Eksp. Khim.*, 2001, vol. 37, no. 3, p. 133.
11. Song, X. and Sayari, A., *Catal. Rev. – Sci. Eng.*, 1996, vol. 38, no. 3, p. 329.
12. Ivanov, A.V. and Kustov, L.M., *Ross. Khim. Zh.*, 2000, vol. 44, no. 2, p. 21.
13. Delahay, G., Ensuque, E., Coq, B., and Figueras, F., *J. Catal.*, 1998, vol. 175, no. 1, p. 7.
14. Pietrogiacomi, D., Tuti, S., Campa, M.C., and Indovina, V., *Book of Abstracts*, 5th Eur. Congr. on Catalysis, Limerik, 2001, p. 48.
15. Struzhko, V.L., Orlik, S.N., Martsenyuk-Kukharuk, M.G., Tel'biz, G.M., Ostapyuk, V.A., and Girushtin, Yu.G., *Teor. Eksp. Khim.*, 1996, vol. 32, no. 5, p. 306.
16. *Practical Surface Analysis by Auger and X-ray Photoelectron Spectroscopy*, Briggs, D. and Seah, M.P., Eds., New York: Wiley, 1983, p. 600.
17. Parvulescu, V.I., Grange, P., and Delmon, B., *Catal. Today*, 1998, vol. 46, p. 233.
18. Mironyuk, T.V., Struzhko, V.L., and Orlik, S.N., *Teor. Eksp. Khim.*, 2000, vol. 36, no. 5, p. 307.
19. Hamada, H., Kintaichi, Y., and Tabata, M., *Chem. Lett.*, 1991, no. 1, p. 217.
20. Zhao, Y., Li, W., Zhang, M., and Tao, K., *Catal. Commun.*, 2002, vol. 3, no. 6, p. 239.
21. Orlik, S.N. and Struzhko, V.L., *Teor. Eksp. Khim.*, 1999, vol. 35, no. 6, p. 373.
22. Nefedov, V.I. *Rentgenoelektronnaya spektroskopiya khimicheskikh soedinenii* (X-ray Electron Spectroscopy of Chemical Compounds), Moscow: Khimiya, 1984.
23. Hu, Z., Allen, F.M., Wan, C.Z., Heck, R.M., Steger, J.J., Lakis, R.E., and Lyman, C.E., *J. Catal.*, 1998, vol. 174, no. 1, p. 13.
24. Harrison, B., Wyatt, M., and Gough, K.G., *Catalysis*, 1982, vol. 5, p. 127.
25. Shelef, M., *Chem. Rev.*, 1995, vol. 95, no. 1, p. 209.
26. Orlik, S.N., Stasevich, V.P., Struzhko, V.L., and Martsenyuk-Kukharuk, M.G., *Teor. Eksp. Khim.*, 1996, vol. 32, no. 4, p. 238.
27. Little, L.H., *Infrared Spectra of Adsorbed Species*, New York: Academic, 1966.
28. Long, R.Q. and Yang, R.T., *J. Phys. Chem.*, 1999, vol. 103, no. 12, p. 2232.
29. Almusaiteer, K.A. and Chuang, S.C., *J. Phys. Chem.*, 2000, vol. 104, no. 10, p. 2265.
30. Sverdlov, L.M., Kovner, M.A., and Krainov, E.P., *Kolebatel'nye spektry molekul* (Vibrational Spectra of Molecules), Moscow: Nauka, 1970.
31. Xin, M., Hwang, I.C., and Woo, S.I., *J. Phys. Chem.*, 1997, vol. 101, no. 44, p. 9005.
32. Kazitsyna, L.A. and Kupletskaya, N.B., *Primenenie UF, IK, YaMR i mass-spektroskopii v organicheskoi khimii* (Applications of UV, IR, NMR, and Mass Spectrometry), Mosocow: Mosk. Gos. Univ., 1979, p. 240.
33. Maisuls, S.E., *Multiphase Catalysts for Selective Reduction of NO_x with Hydrocarbons*, 2000.
34. Orlik, S.N., Struzhko, V.L., Mironyuk, T.V., and Tel'biz, G.M., *Teor. Eksp. Khim.*, 2001, vol. 37, no. 5, p. 306.
35. Davydov, A.A., *IK-spektroskopiya v khimii poverkhnosti okislov* (IR Spectroscopy Applied to the Chemistry of Oxide Surfaces), Novosibirsk: Nauka, 1984.
36. Matyshak, V.A. and Krylov, O.V., *Catal. Today*, 1995, vol. 25, p. 1.
37. Hopstaken, M.J.P. and Niemantsverdriet, J.W., *J. Phys. Chem.*, 2000, vol. 104, no. 14, p. 3058.
38. Daturi, M., Finnocchio, E., Binet, C., Lavalley, J.-C., Fally, F., Perrichon, V., Vidal, H., Hickey, N., and Kaspar, J., *J. Phys. Chem.*, 2000, vol. 104, no. 39, p. 9186.
39. Fornasiero, P., Ranga Rao, G., Kaspar, J., L'Erario, F.L., and Graziani, M., *J. Catal.*, 1998, vol. 175, no. 2, p. 269.